

Supporting information

Efficient Synthesis of Vinylene-Linked Conjugated Porous Networks via the Horner-Wadsworth-Emmons Reaction for Photocatalytic Hydrogen evolution

Yanyan He¹, Wangping Ma¹, Na Yang³, Fulai Liu², Yong Chen², Honglai Liu*¹, Xiang Zhu*³

¹ State Key Laboratory of Chemical Engineering, School of Chemical Engineering,
East China University of Science and Technology, Shanghai, 200237, China

² Key Laboratory of Photochemical Conversion and Optoelectronic Materials,
HKU-CAS Joint Laboratory on New Materials, Technical Institute of Physics and Chemistry,
Chinese Academy of Sciences, Beijing 100190, China

³ State Key Laboratory for Oxo Synthesis and Selective Oxidation,
Suzhou Research Institute of Lanzhou Institute of Chemical Physics,
Chinese Academy of Sciences, Suzhou 215000, China

General experimental methods

Materials.

Trifluoromethanesulfonic acid and 1,3,5-Triformylbenzene (BF) was purchased from Macklin. Benzoyl peroxide was purchased from TCI. Trimethyl phosphite, N-bromosuccinimide, *p*-tolunitrile, benzaldehyde and potassium tert-butoxide was purchased from Adamas-beta. All the general solvents used were purchased from Adamas-beta General Reagent. Extra Dry N, N-Dimethylformamide and dichloromethane was purchased from Meryer. 1,3,5-tris(4-formylphenyl) benzene (TBF) and 2,4,6-Tris(4-formylphenyl)-1,3,5-triazine (TTF) were synthesized following reported procedure.^{1,2} The reactions were performed using standard Schlenk vacuum-line techniques under nitrogen atmosphere.

Instrumentation

Liquid nuclear magnetic resonance (¹H NMR and ¹³C NMR) spectra were measured on Bruker Ascend 400 and Ascend 600 spectrometer using chloroform-d and dichloromethane-d as solvent and tetramethylsilane ($\delta = 0$) as internal reference. Solid-state ¹³C NMR experiments were performed on a Bruker AVANCE III 500 spectrometer. Mass spectra were carried out on a Waters ESI- high-resolution orthogonal acceleration time-of-flight mass spectrometry (Xevo G2 TOF MS) using acetonitrile as a matrix. Fourier transform infrared spectroscopy (FT-IR) recorded with a Nicolet iS 10 (Thermo Fisher). Attenuated total reflectance Fourier transform infrared (ATR FT-IR) spectrometer, the samples for IR test were prepared as KBr pellets. Powder X-ray diffraction patterns were recorded in transmission geometry using a Rigaku Smart Lab X-ray diffractometer over the 2θ range from 5° to 80° with a scanning speed of 5° min^{-1} . DRS UV-Vis absorption spectra were recorded at room temperature on a Lambda 950* Spectrophotometer. Fluorescence spectroscopy (PL) spectra were obtained with a FLS 1000 spectrophotometer. Thermal gravimetric analysis (TGA) was performed on a TGA 8000 thermo-gravimetric analyzer to investigate the thermal stability of all samples in nitrogen atmosphere from ambient temperature to 800°C at the rate of $20^\circ \text{C min}^{-1}$. X-ray photoelectron spectroscopy (XPS) measurements were tested on ESCALAB 250Xi instrument (Thermo Fisher) using a monochromatic Al Ka x-ray source. Ultraviolet photoelectron spectroscopy (UPS) measurements were performed with an unfiltered HeI (21.22 eV) gas discharge lamp and a total instrumental energy resolution of 100 meV. The gas sorption isotherms were measured via a 3Flex-Surface Characterization Analyzer based on N₂ adsorption and desorption. Samples were degassed at 120°C for 6 h under vacuum before analysis. SEM measurements were performed on a S-3400N field emission scanning electron microscope. TEM

characterizations were conducted using a JEM-1400 (JEOL Ltd., Japan) with an accelerating voltage of 100 KV. Theoretical calculations were performed on the Gaussian 09 program. The B3LYP functions and the 6-31 G(d) basis set were used for all the atoms in the DFT calculations. Pt containing was detected by Inductively Coupled Plasma Atomic Emission Spectrometer (ICP-AES, 167 nm-785 nm/725, Agilent).

Photocatalytic H₂ Evolution.

Photocatalyst powder (25 mg) was first dispersed in 25 mL 0.2 M Ascorbic acid (AA) aqueous solution in an online photocatalytic hydrogen production system (Labsolar-6A, PerfectLight of Beijing). The dispersion was ultrasonicated for 30 minutes. 1 mL 2 mg/ml H₂PtCl₆ · 6H₂O (3 wt% Pt) was introduced as the precursor to Pt cocatalyst deposition on surface. The solution was then carefully evacuated to remove air and filled with Ar. For photocatalytic experiments, the solution was directly irradiated by a 300 W Xe-lamp with a cutoff filter ($\lambda > 420$ nm). The reaction temperature was maintained at 5.5 °C by a water-cooling system. The amount of H₂ was determined using an on-line gas chromatograph (GC-2014C, Shimadzu).

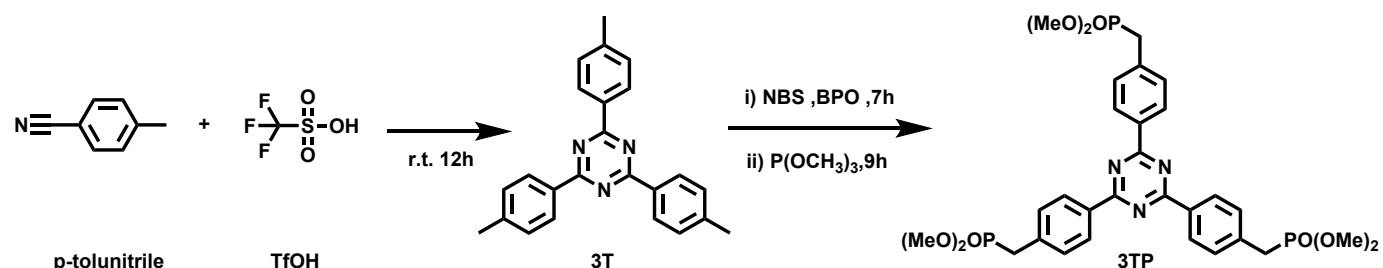
AQY measurement:

The apparent quantum efficiency (AQE) was measured under the illumination of a 300 W Xe lamp with different band-pass filters for 2 hours, which was calculated using the following formula:

$$\begin{aligned} \text{AQE} &= \frac{2 \times \text{the number of evolved H}_2 \text{ molecules}}{\text{the number of incident photons}} \times 100\% \\ &= \frac{2 \times n_{\text{H}_2} \times N_A \times h \times c}{I \times S \times t \times \lambda} \end{aligned}$$

n_{H_2} is the amount of H₂ molecules, N_A is Avogadro constant, h is the Planck constant, c is the speed of light, I is the intensity of irradiation light, S is the irradiation area, t is the photoreaction time, and λ is the wavelength of the monochromatic light.

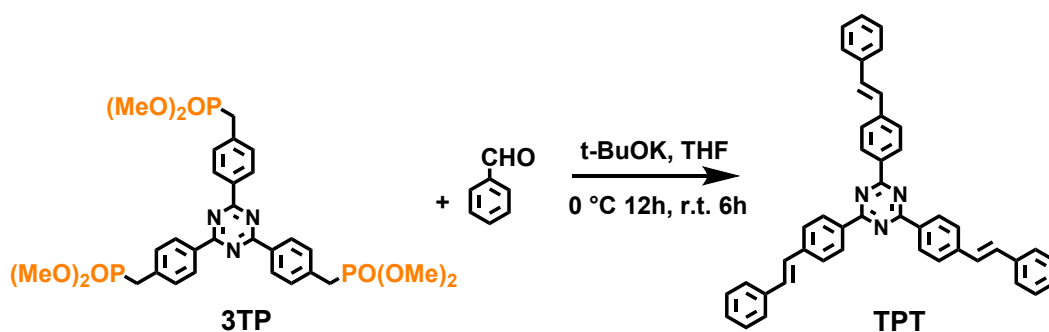
1. Synthetic procedures:



Scheme S1. Synthetic routes for the monomers.

2,4,6-tri (p-tolyl)-1,3,5-triazine (3T):³ In a 250 mL flask, *p*-tolunitrile (94.21 mmol, 1 equiv.) was dissolved in dry dichloromethane (80 ml). Trifluoromethanesulfonic acid (282.62 mmol, 3 equiv.) was slowly added to this solution at 0 °C. The mixture was stirred at room temperature for 12 h, then poured into ice water and neutralized with ammonium hydroxide. The precipitate was filtered out and then washed with water and acetone for several times. Then the compound was recrystallized from toluene to deliver white acicular solid with a yield of 68%. ¹H NMR (400 MHz, CDCl₃) δ (ppm): 8.71-8.56 (m, 1H), 7.36 (d, 1H), 2.47 (s, 2H).

(4,4',4''-(1,3,5-Triazine-2,4,6-triyl)tris(benzene-4,1-diyl))tris(methylene)triphosphonate (3TP):⁴ In a 100 mL round-bottom flask, 2,4,6-Tri(*p*-tolyl)-1,3,5-triazine (3.51 g, 0.01 mol), NBS (5.34 g, 0.03 mol) and BPO (0.3 g, 1.2 mmol) were dissolved into 50 mL chlorobenzene and heated at 110°C for 7 h. The mixture was filtered and the solvent was removed under vacuum. The residue was dissolved into trimethyl phosphite (10 mL) and refluxed for 9 h. The excessive trimethyl phosphite was removed under vacuum. The residue was purified by column chromatography on silica (tetrahydrofuran) to afford the product as white powder in 55% yield. ¹H NMR (400 MHz, CDCl₃) δ (ppm): 8.76-8.65 (m, 1H), 7.51 (d, 1H), 3.71 (d, 3H), 3.31 (d, 1H). ¹³C NMR (400 MHz, CDCl₃) δ (ppm) 171.29, 136.27, 136.18, 135.04, 135.00, 130.12, 130.05, 129.26, 129.23, 53.08, 53.01, 33.90, 32.53.



Scheme S2. Synthesis of model compound by HWE reaction.

Model compound (TPT):⁵ In a 50 mL Schlenk flask, 3TP (100 mg, 0.16 mmol) and Benzaldehyde (49 μ L, 0.48 mmol) were dissolved in anhydrous DMF (10 mL) under the protection of nitrogen. After the mixture was cooled in an ice-water bath, *t*-BuOK (107 mg, 0.96 mmol) was added rapidly. Then the reaction was left overnight in ice-bath. The mixture was warmed to room temperature and stirred for another 4 hours, then washed with water and dichloromethane. The combined organic layer was dried over anhydrous MgSO₄ and concentrated using a rotary evaporator. The residue was purified by column chromatography on silica (petroleum ether/dichloromethane=3:1, v/v) to yield the product as yellow powder (48 mg, yield: 49%). ¹H NMR (400 MHz, CDCl₃) δ (ppm): 8.74 (d, 1H), 7.69 (d, 1H), 7.58 (d, 1H), 7.39 (t, 1H), 7.36 – 7.26 (m, 1H), 7.20 (d, J = 16.3 Hz, 1H). ¹³C NMR (400 MHz, CD₂Cl₂) δ (ppm): 170.30, 140.76, 136.25, 134.59, 129.90, 128.53, 128.02, 127.37, 127.10, 126.00, 125.92. MS(ESI): Calcd for C₄₅H₃₃N₃ 615.2674; found 615.2751(M⁺H)⁺.

CPN-1: In a 50 mL Schlenk flask, 3TP (100 mg, 0.16 mmol) and benzene-1,3,5-trialdehyde (26 mg, 0.16 mmol) were dissolved in anhydrous DMF (10 mL) under the protection of nitrogen. After the mixture was cooled with ice, *t*-BuOK (107 mg, 0.96 mmol) was added slowly. Then the mixture stirred for 12 h with an ice-bath. The mixture was warmed to room temperature and stirred for another 6 h. The insoluble precipitated network polymer was filtered and washed with DMF (50 mL, three times), THF (50 mL, three times), ethanol (50 mL, three times), and dichloromethane (50 mL, three times) to remove any unreacted monomers or catalyst residues. The residual solid was dried under vacuum for 24 h at 60 °C to give yellow powder with 86% yield.

CPN-2: To a 50 mL Schlenk bottle, 3TP (100 mg, 0.16 mmol) and 1,3,5-tris(4-formylphenyl) benzene (TBF) (62 mg, 0.16 mmol) and anhydrous DMF (10 mL) were added under the protection of nitrogen. After the mixture was cooled down with ice, *t*-BuOK (107 mg, 0.96 mmol) was added. Then the mixture was kept in ice-bath. After stirring 12 h, the mixture was warmed to room temperature and stirred for another 6 h. The insoluble precipitated network polymer was filtered and washed with DMF (50 mL, three times), THF (50 mL, three times), ethanol (50 mL, three times), and dichloromethane (50 mL, three times) to remove any unreacted monomers or catalyst residues. The residual solid was dried under vacuum for 24 h at 60 °C to give yellow powder with 90% yield.

CPN-3: 3TP (100 mg, 0.16 mmol) and 2,4,6-Tris(4-formylphenyl)-1,3,5-triazine (TTF) (63 mg, 0.16 mmol) were filled into a 50 mL Schlenk flask, followed by the addition of anhydrous DMF (10 mL) under

nitrogen. After the mixture was cooled down, *t*-BuOK (107 mg, 0.96 mmol) was added. Then the mixture was kept in ice-bath and stirred for 12 h. After that, the mixture was warmed to room temperature, stirring for another 6 h. The insoluble precipitates were filtered and washed with DMF (50 mL, three times), THF (50 mL, three times), ethanol (50 mL, three times), and dichloromethane (50 mL, three times) to remove any un-reacted monomers or catalyst residues. The residual solid was dried under vacuum for 24 h at 60 °C to deliver yellow powder with 86% yield.

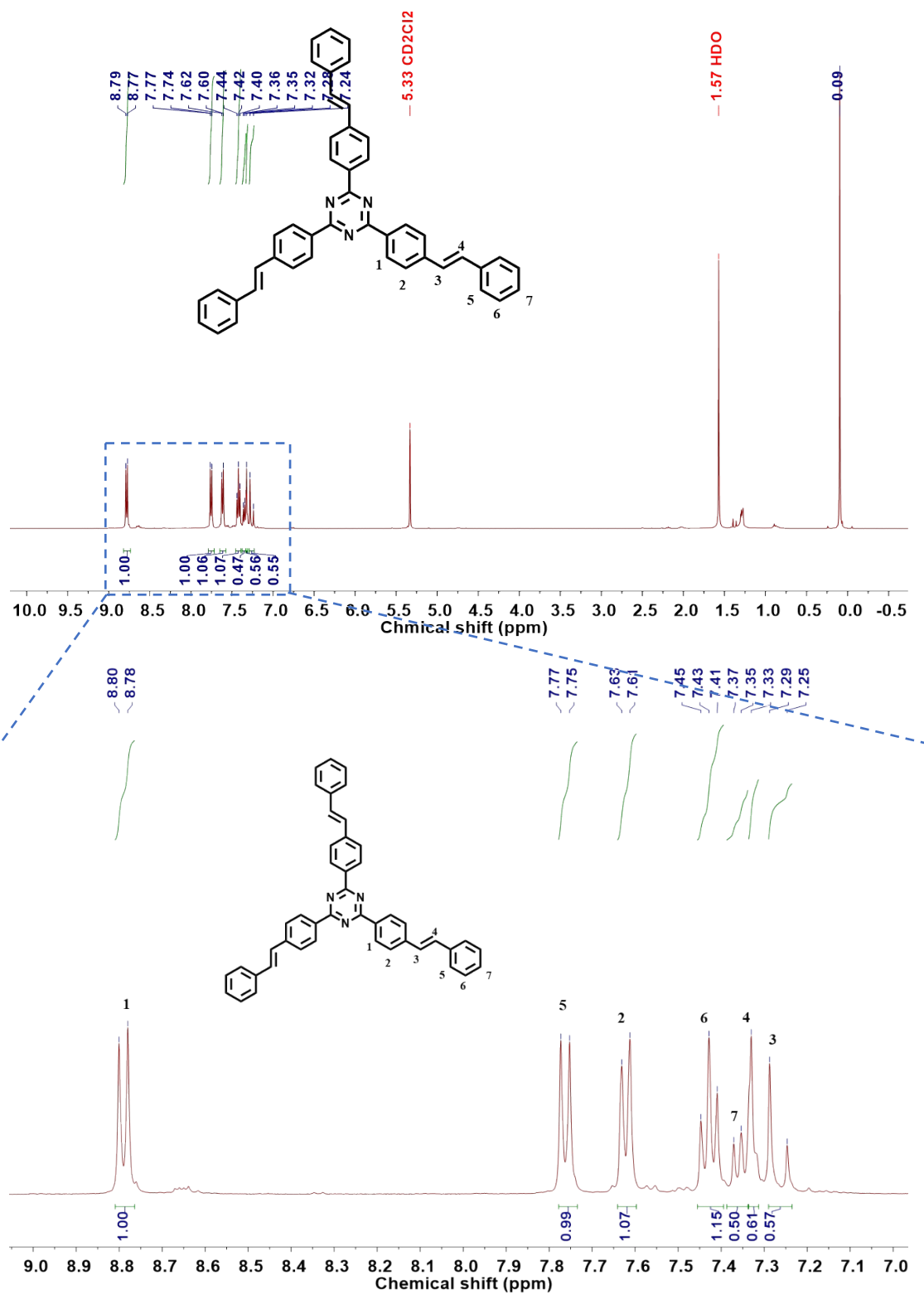


Figure S1. ^1H NMR (CD_2Cl_2 , 400 MHz) spectrum of TPT.

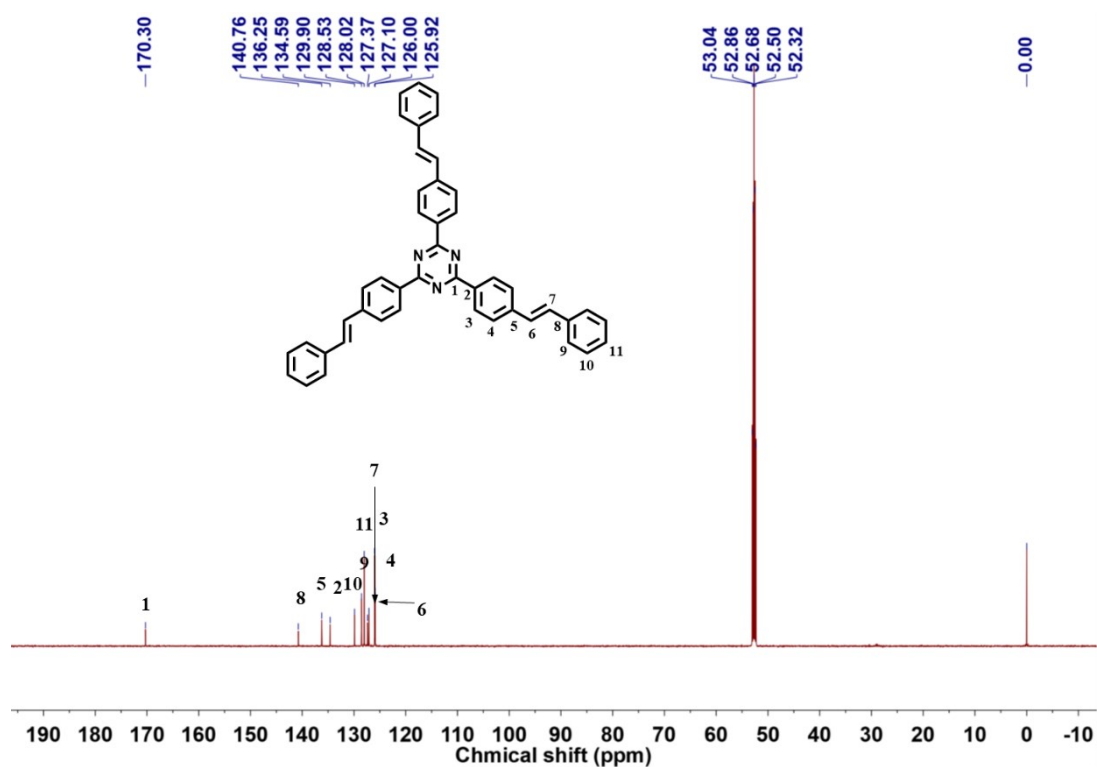


Figure S2. ^{13}C NMR (CD_2Cl_2 , 151 MHz) spectrum of TPT.

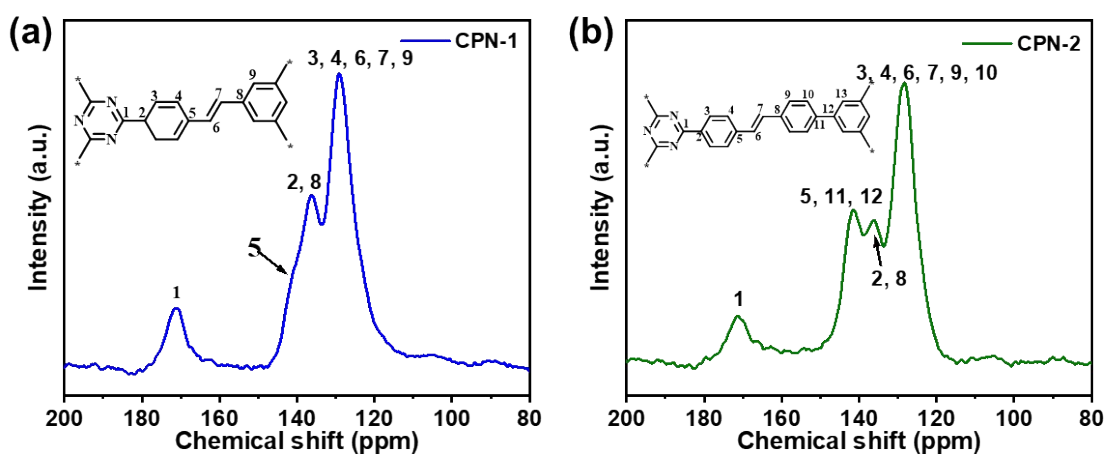


Figure S3. Solid-state ^{13}C CP/MAS NMR spectra of CPN-1 and CPN-2.

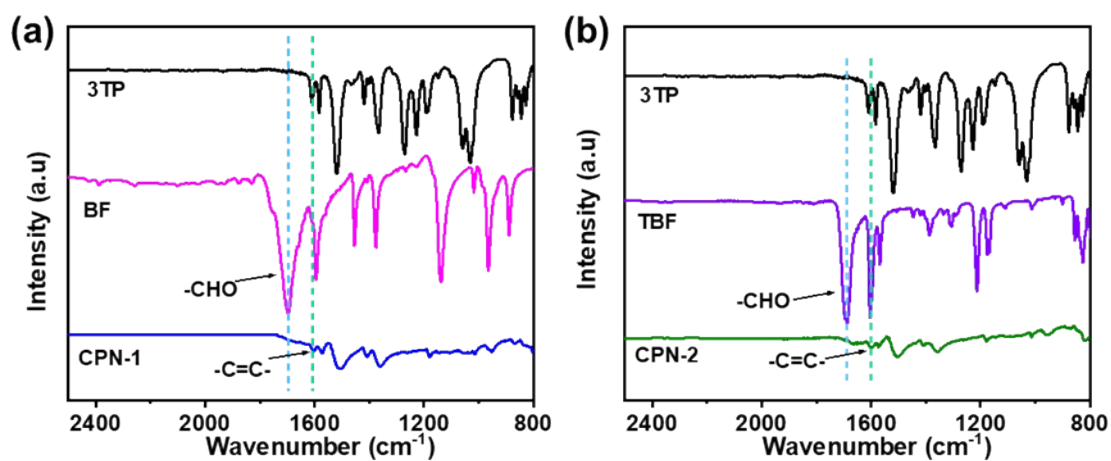


Figure S4. Transmission FT-IR spectra of CPNs and corresponding monomers as KBr pellets.

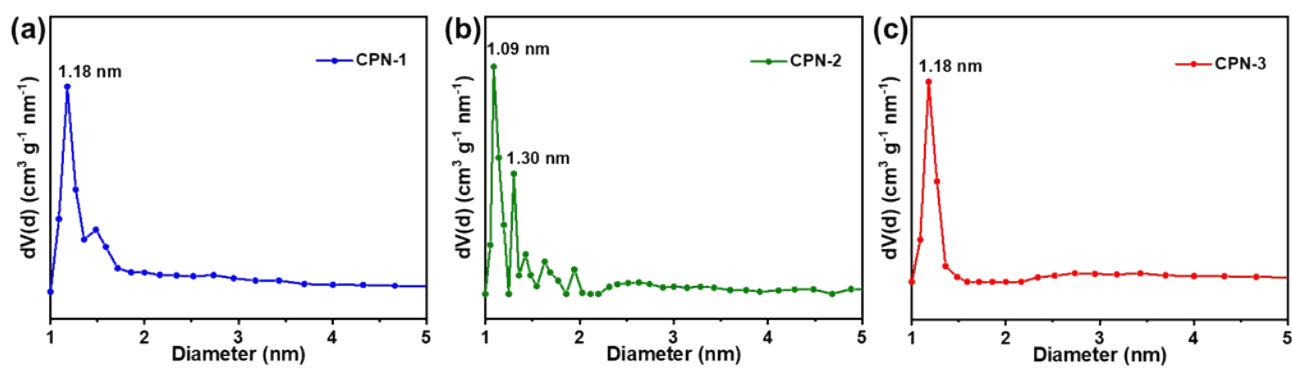


Figure S5. The calculated pore size distributions of CPNs.

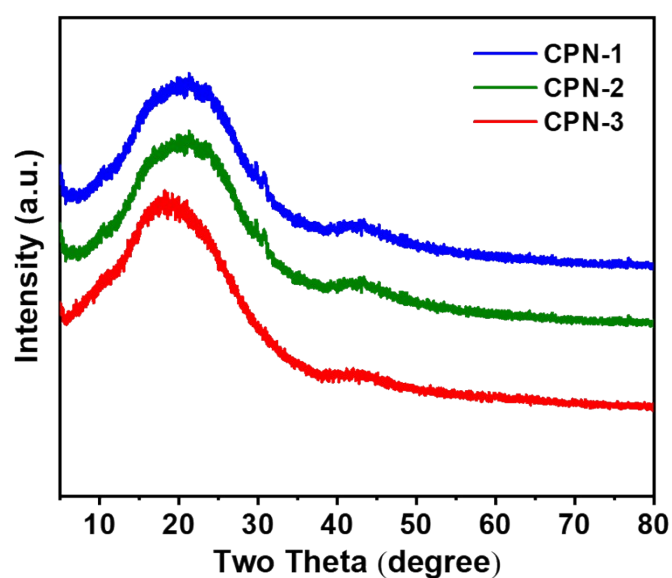


Figure S6. Experimentally observed PXRD patterns of CPNs.

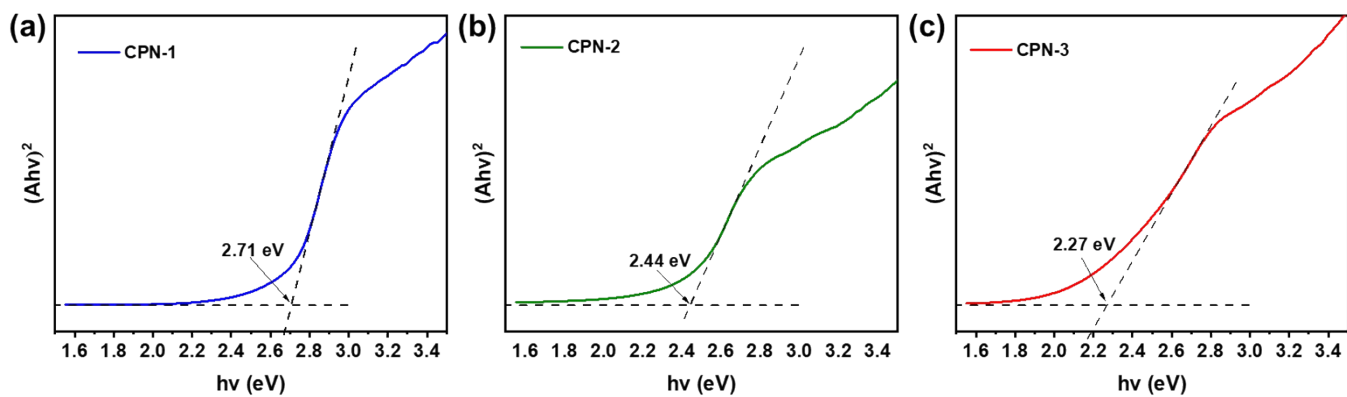


Figure S7. Band gaps of the CPNs determined from the Kubelka-Munk transformed reflectance spectra.

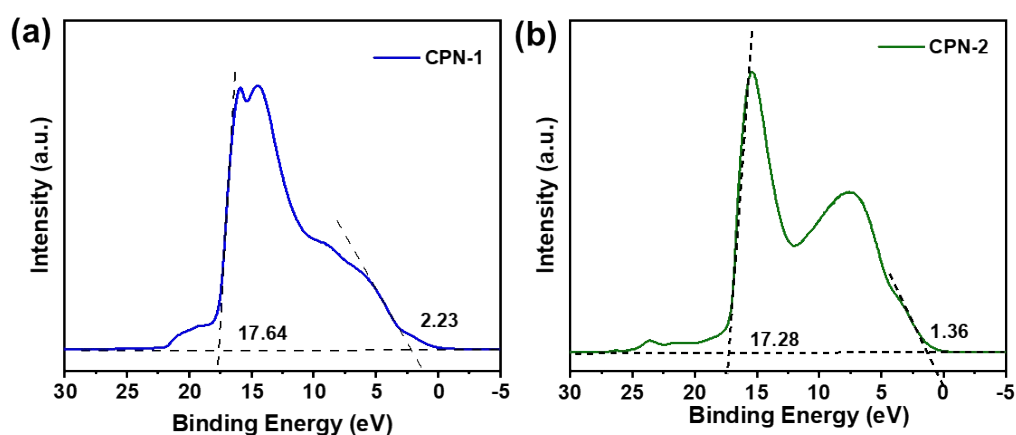


Figure S8. UPS spectra of CPNs (solid curve). The dashed lines mark the baseline and the tangents of the curves. The intersections of the tangents with the baseline give the edges of the UPS spectra from which the UPS width is determined.

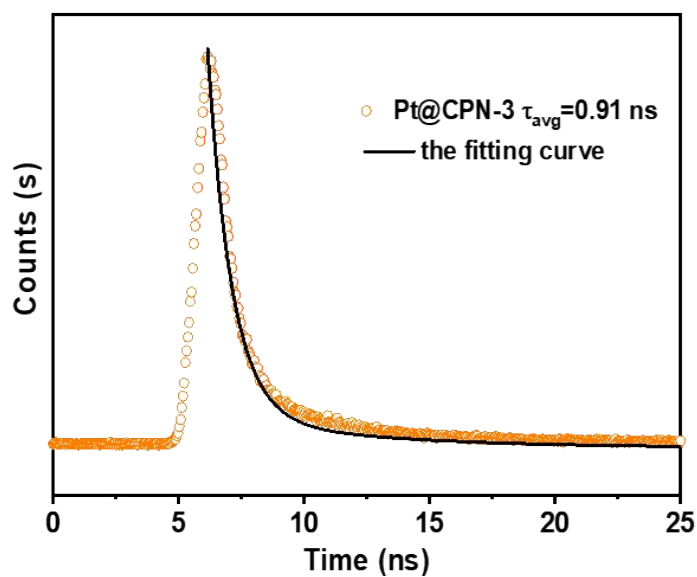


Figure S9. Time-resolved transient photoluminescence (PL) decay of CPN-3 loaded with Pt.

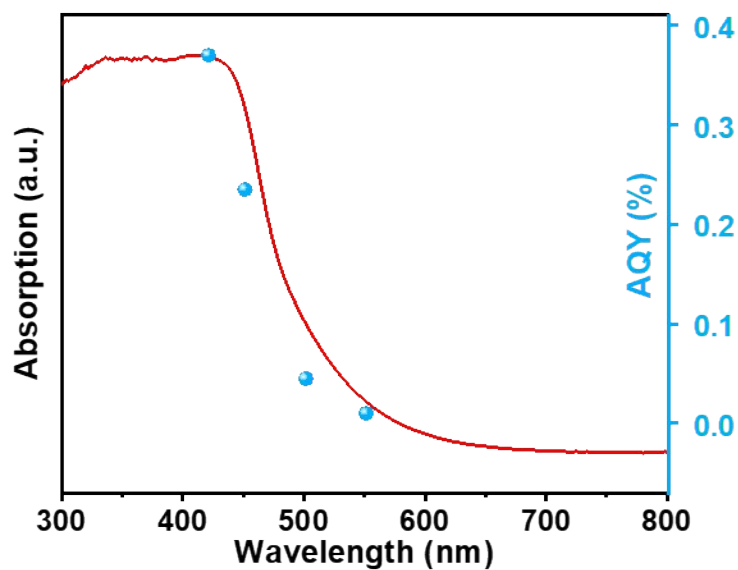


Figure S10. Overlay of UV/Vis absorption spectra of CPN-3 and the corresponding apparent quantum yield (AQY).

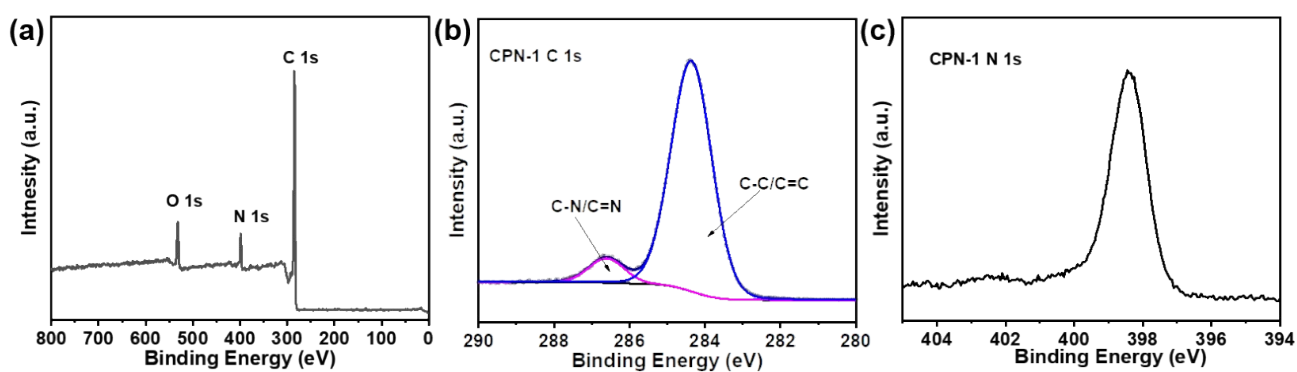


Figure S11. XPS analysis of CPN-1.

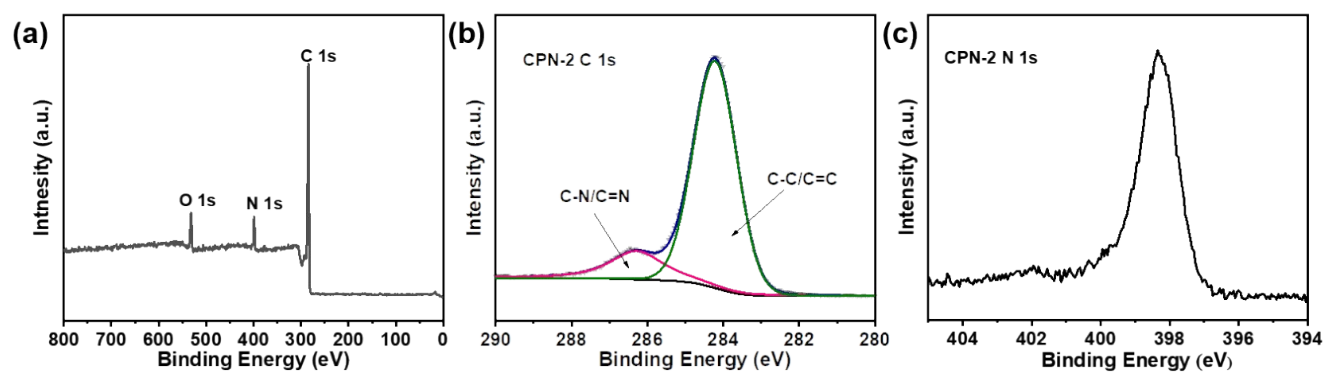


Figure S12. XPS analysis of CPN-2.

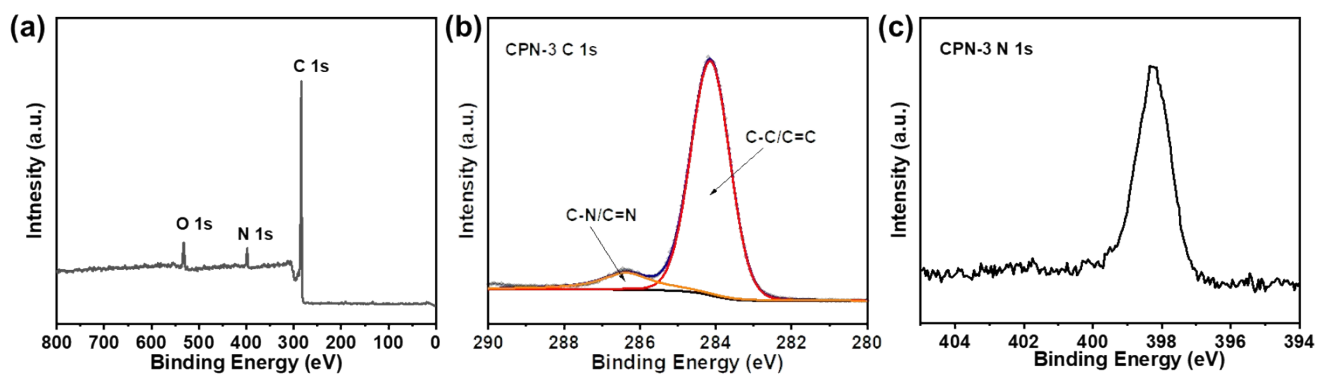


Figure S13. XPS analysis of CPN-3.

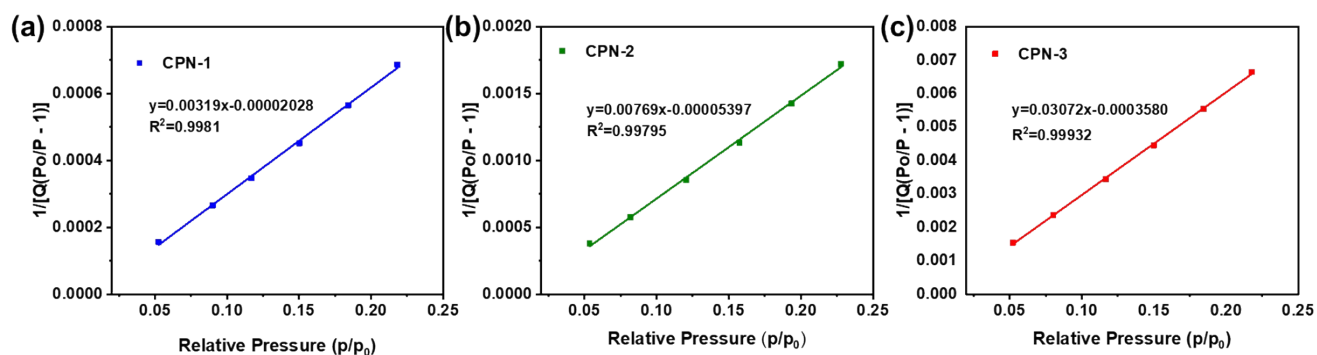


Figure S14. BET plots ($P/P_0 = 0.06-0.2$) from N_2 isotherms at 77 K.

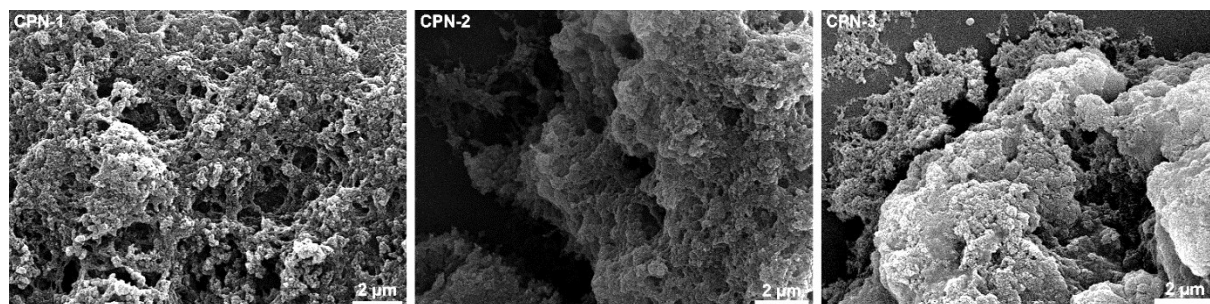


Figure. S15 SEM images of CPNs.

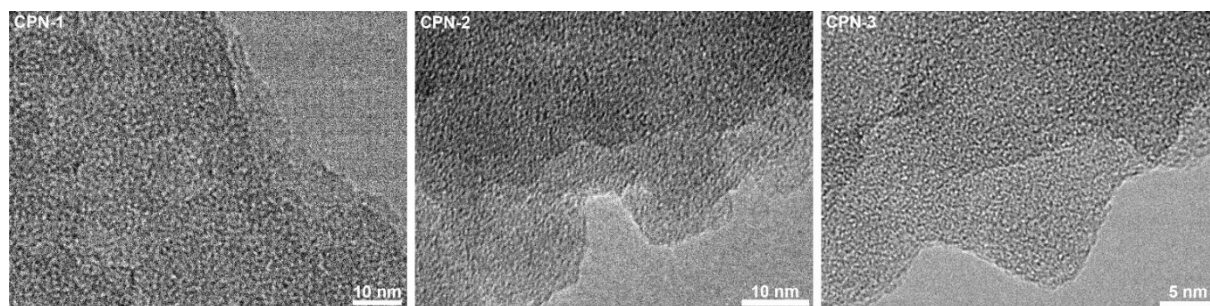


Figure. S16 TEM images of the polymers of CPNs.

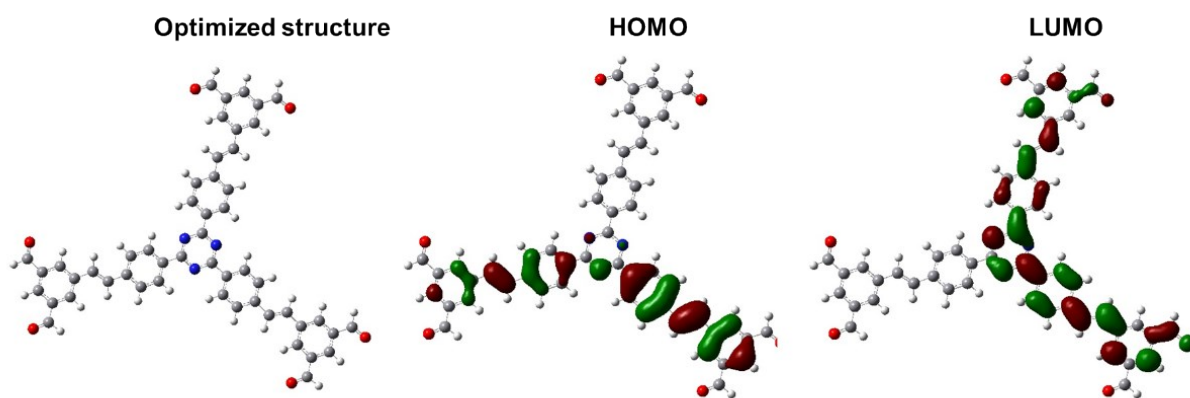


Figure S17. Molecular orbital diagrams of CPN-1 from DFT calculation.

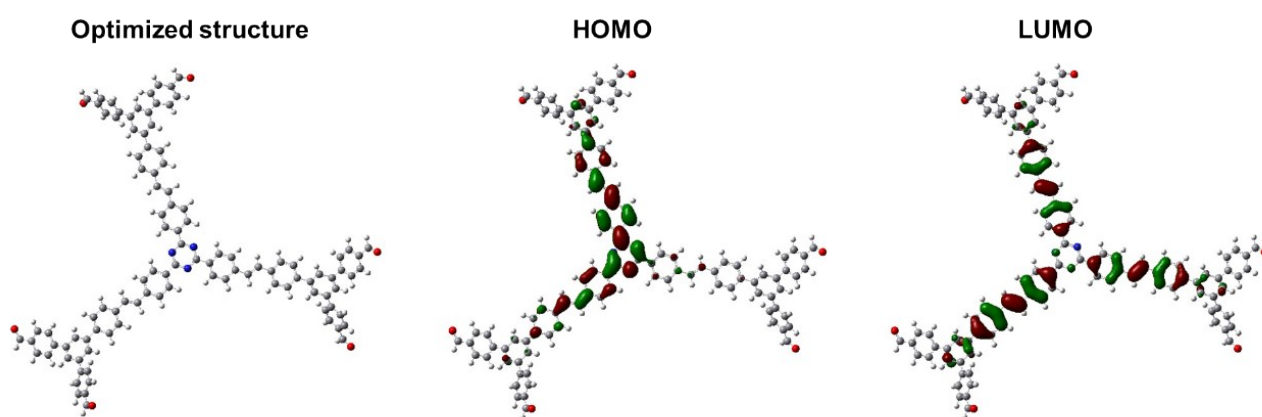


Figure S18. Molecular orbital diagrams of CPN-2 from DFT calculation.

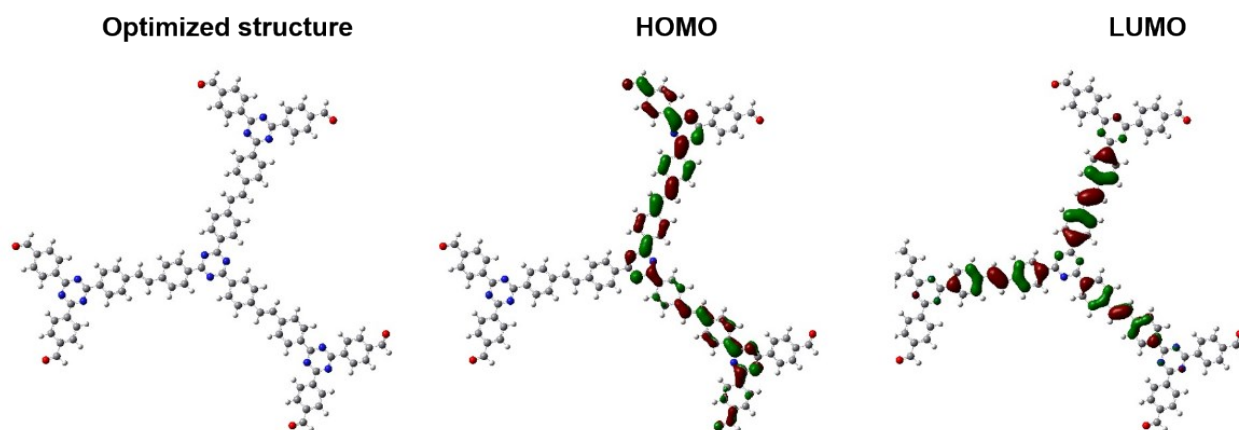


Figure S19. Molecular orbital diagrams of CPN-3 from DFT calculation.

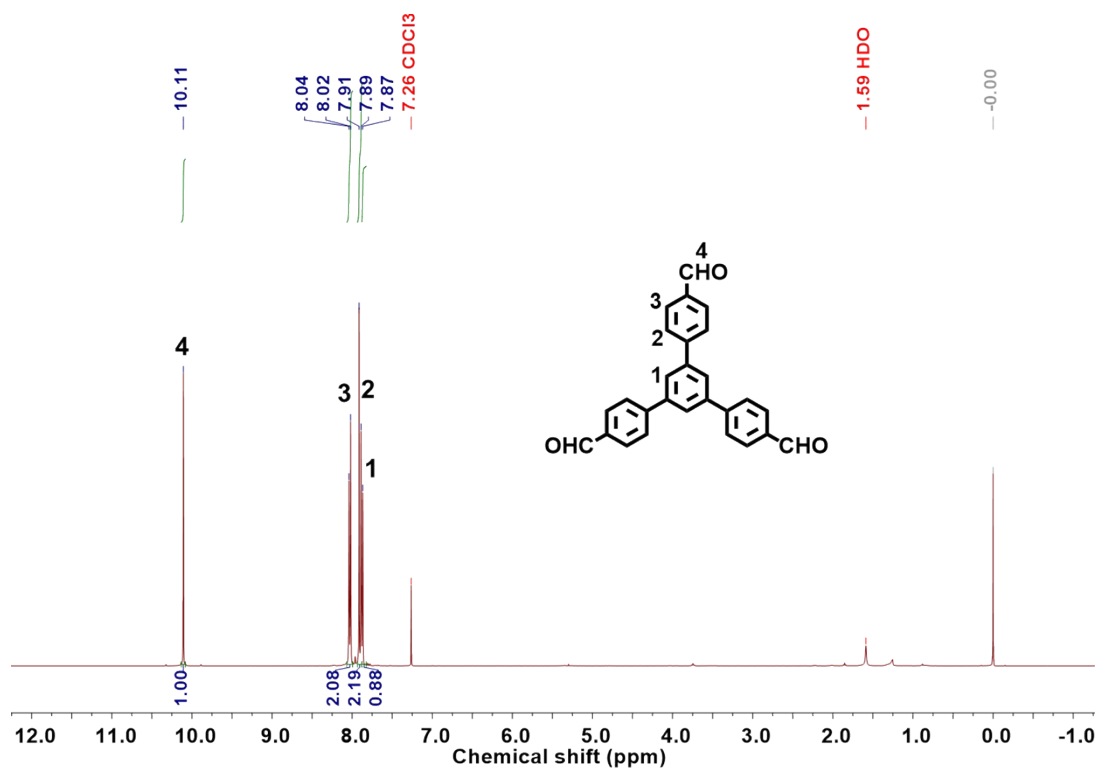


Figure S20. ^1H NMR (CDCl₃, 400 MHz) of TBF.

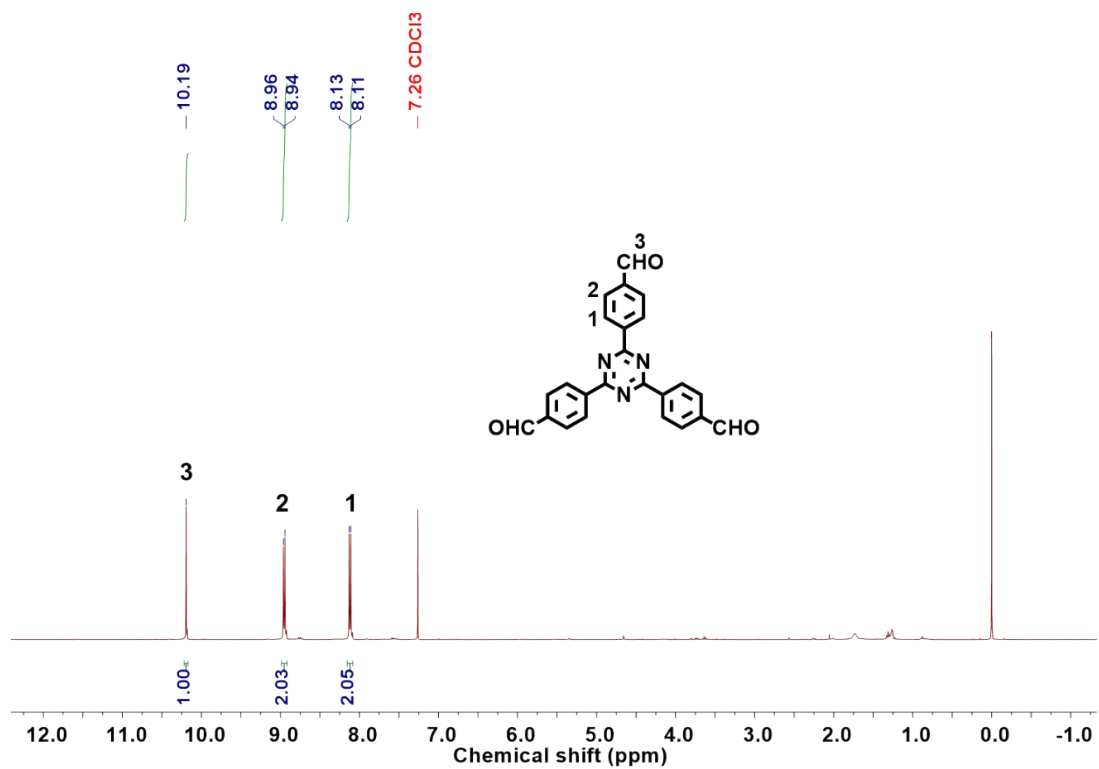


Figure S21. ^1H NMR (CDCl₃, 400 MHz) of TTF.

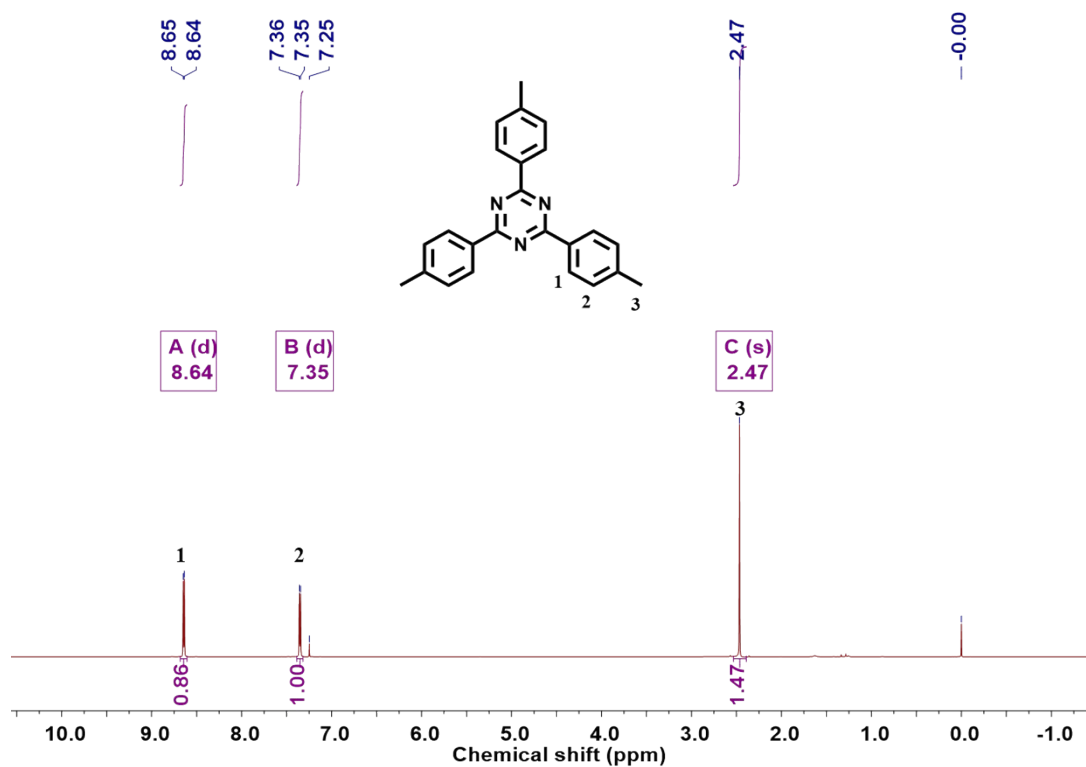


Figure S22. ¹H NMR (CDCl₃, 600 MHz) spectrum of 3T.

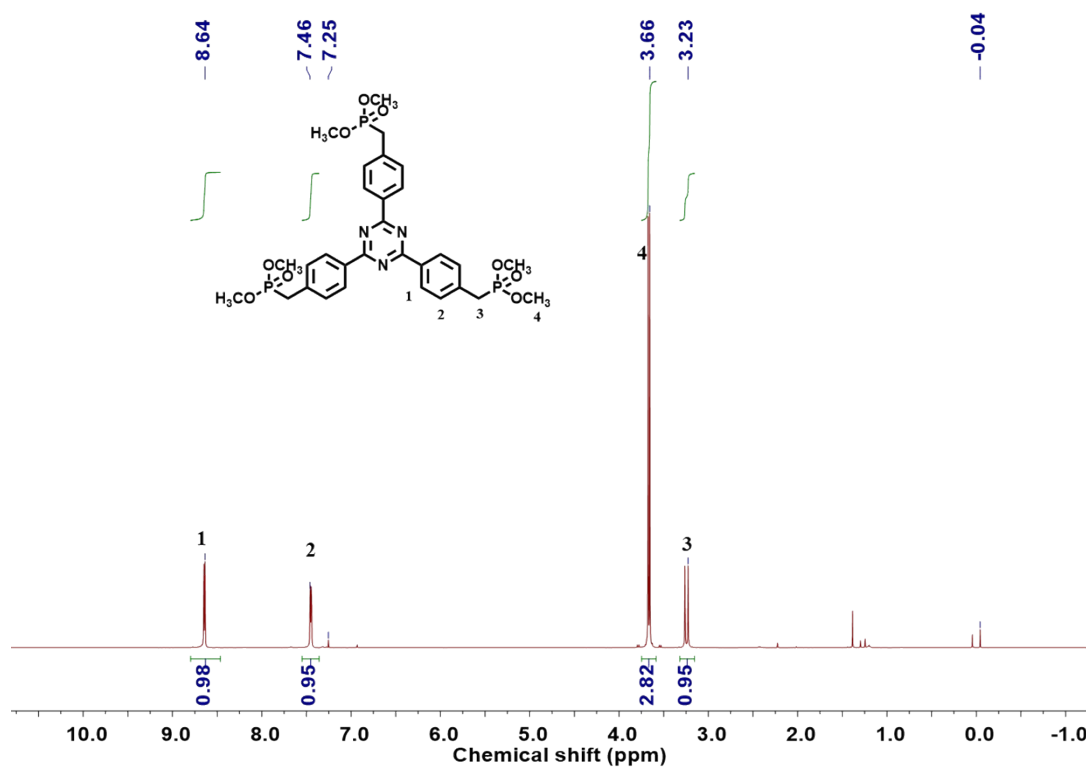


Figure S23. ¹H NMR (CDCl₃, 600 MHz) spectrum of 3TP.

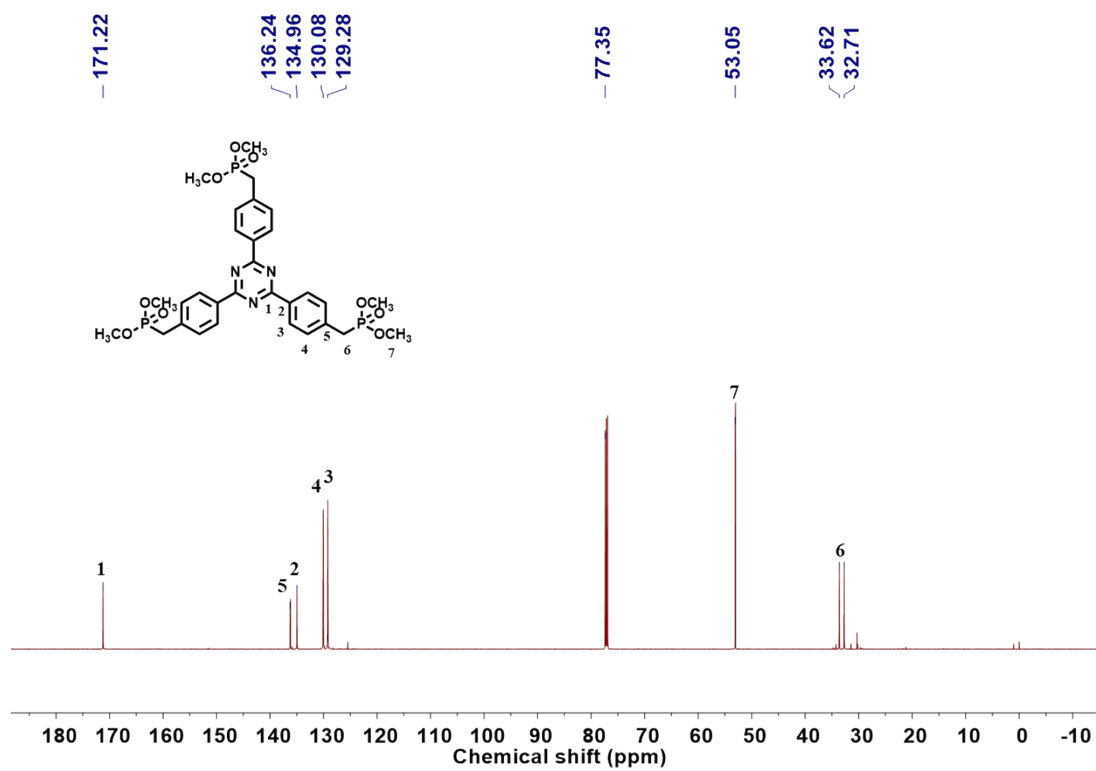


Figure S24. ^{13}C NMR (CDCl_3 , 125 MHz) spectrum of **3TP**.

Table S1. Comparison of photocatalytic activity with different polymer photocatalysts reported in literature.

Photocatalysts	Cocatalyst	Sacrificial donor ^a	Irradiance	H ₂ evolution (μmol h ⁻¹ g ⁻¹)	AQY	Reference
CPN-3	3 wt% Pt	AA	≥420 nm	1508	0.37% (420 nm)	This work
CN-NaK	3 wt% Pt	TEOA	≥420 nm	5560	60% (420 nm)	6
PyBS-3	3 wt% Pt	AA	≥300 nm	105000	29.3% (420 nm)	7
P64	8 wt% Pt	TEA	≥420 nm	6038.5	20.7% (420 nm)	8
TFPT-COF	2.2 wt% Pt	TEOA	≥ 420 nm	1900	2.2% (420 nm)	9
N ₃ -COF	3 wt% Pt	TEOA	≥ 420 nm	1700	no	10
L-PyBT	3 wt% Pt	TEOA	≥ 420 nm	1674	no	11
CPCN-1*	3 wt% Pt	TEOA	≥ 420 nm	1493	2.14% (420 nm)	12
sp ² c-COF	3 wt% Pt	TEOA	≥420 nm	1360	0.46 (420 nm)	13
CTF-1_10 min	Pt	TEOA	≥420 nm	1072	6.4% (450 nm)	14
OB-POP-3	3 wt% Pt	TEOA	≥420 nm	908	2.0% (420 nm)	15
g-C ₃ N ₄ /CTF-1	3 wt% Pt	TEOA	≥ 420 nm	850	no	16
PMPA-250	3 wt% Pt	TEOA	≥ 420 nm	584	1.1% (432 nm)	17
C ₃ N _{4+x}	3 wt% Pt	TEOA	≥ 400 nm	554	~0.7% (350 nm)	18
TFPT-OCH ₃	3 wt% Pt	TEOA	≥420 nm	442	1.03% (405 nm)	19
P12	No	TEA	≥ 420 nm	420	1.4% (420 nm)	20
A1/D1 NADHs (70.6 wt% A1)	9 wt% Pt	AA	≥ 420 nm	383	3.72% (420 nm)	21
TP-BDDA	3 wt% Pt	TEOA	≥ 395 nm	324	1.3% (420 nm)	22
PyBT-2	3 wt% Pt	TEOA	≥ 420 nm	296	1.0% (420 nm)	23
g-C ₁₈ N ₃ -COF	3 wt% Pt	AA	≥ 420 nm	292	1.06% (420 nm)	24
CP-CMP10	3 wt% Pt	DEA	≥ 420 nm	190	4.2% (310 nm, 430 nm)	25

^a TEOA: triethanolamine; TEA: trimethylamine; DEA: diethylamine; AA: ascorbic acid.

Reference

1. S. Jiang, J. Bacsá, X. Wu, J. T. A. Jones, R. Dawson, A. Trewin, D. J. Adams and A. I. Cooper, *Chem. Commun.*, 2011, **47**, 8919-8921.
2. A. K. Sekizkardes, S. Altarawneh, Z. Kahveci, T. İslamođlu and H. M. El-Kaderi, *Macromolecules*, 2014, **47**, 8328-8334.
3. Z. Lin, T. J. Emge and R. Warmuth, *Chemistry*, 2011, **17**, 9395-9405.
4. Y. Jiang, Y. Wang, B. Wang, J. Yang, N. He, S. Qian and J. Hua, *Chem. Asian J.*, 2011, **6**, 157-165.
5. Y. Jiang, Y. Wang, J. Hua, J. Tang, B. Li, S. Qian and H. Tian, *Chem. Commun.*, 2010, **46**, 4689-4691.
6. G. Zhang, L. Lin, G. Li, Y. Zhang, A. Savateev, S. Zafeiratos, X. Wang and M. Antonietti, *Angew. Chem. Int. Ed.*, 2018, **57**, 9372-9376.
7. C. Shu, C. Han, X. Yang, C. Zhang, Y. Chen, S. Ren, F. Wang, F. Huang and J.-X. Jiang, *Adv. Mater.*, 2021, 2008498.
8. Y. Bai, L. Wilbraham, B. J. Slater, M. A. Zwijnenburg, R. S. Sprick and A. I. Cooper, *J. Am. Chem. Soc.*, 2019, **141**, 9063-9071.
9. L. Stegbauer, K. Schwinghammer and B. V. Lotsch, *Chem. Sci.*, 2014, **5**, 2789-2793.
10. V. S. Vyas, F. Haase, L. Stegbauer, G. Savasci, F. Podjaski, C. Ochsenfeld and B. V. Lotsch, *Nat. Commun.*, 2015, **6**, 8508.
11. C. Cheng, X. Wang, Y. Lin, L. He, J.-X. Jiang, Y. Xu and F. Wang, *Polym. Chem.*, 2018, **9**, 4468-4475.
12. H. Wang, B. Wang, Y. Bian and L. Dai, *ACS Appl Mater Interfaces*, 2017, **9**, 21730-21737.
13. E. Jin, Z. Lan, Q. Jiang, K. Geng, G. Li, X. Wang and D. Jiang, *Chem.*, 2019, **5**, 1632-1647.
14. S. Kuecken, A. Acharjya, L. Zhi, M. Schwarze, R. Schomacker and A. Thomas, *Chem. Commun.*, 2017, **53**, 5854-5857.
15. S. Bi, Z.-A. Lan, S. Paasch, W. Zhang, Y. He, C. Zhang, F. Liu, D. Wu, X. Zhuang, E. Brunner, X. Wang and F. Zhang, *Adv. Funct. Mater.*, 2017, **27**, 1703146.
16. G. Zhou, L. L. Zheng, D. Wang, Q. J. Xing, F. Li, P. Ye, X. Xiao, Y. Li and J. P. Zou, *Chem. Commun.*, 2019, **55**, 4150-4153.
17. X. Huang, Z. Wu, H. Zheng, W. Dong and G. Wang, *Green Chem.*, 2018, **20**, 664-670.
18. J. Fang, H. Fan, M. Li and C. Long, *J. Mater. Chem. A*, 2015, **3**, 13819-13826.
19. K. Yu, S. Bi, W. Ming, W. Wei, Y. Zhang, J. Xu, P. Qiang, F. Qiu, D. Wu and F. Zhang, *Polym. Chem.*, 2019, **10**, 3758-3763.
20. R. S. Sprick, Catherine M. Aitchison, E. Berardo, L. Turcani, L. Wilbraham, B. M. Alston, K. E. Jelfs, M. A. Zwijnenburg and A. I. Cooper, *J. Mater. Chem. A*, 2018, **6**, 11994-12003.
21. H. Yang, X. Li, R. S. Sprick and A. I. Cooper, *Chem. Commun.*, 2020, **56**, 6790-6793.
22. P. Pachfule, A. Acharjya, J. Roeser, T. Langenhahn, M. Schwarze, R. Schomacker, A. Thomas and J. Schmidt, *J. Am. Chem. Soc.*, 2018, **140**, 1423-1427.
23. Y. Xu, N. Mao, C. Zhang, X. Wang, J. Zeng, Y. Chen, F. Wang and J.-X. Jiang, *Appl. Catal. B-Environ.*, 2018, **228**, 1-9.
24. S. Wei, F. Zhang, W. Zhang, P. Qiang, K. Yu, X. Fu, D. Wu, S. Bi and F. Zhang, *J. Am. Chem. Soc.*, 2019, **141**, 14272-14279.

25. R. S. Sprick, J. X. Jiang, B. Bonillo, S. Ren, T. Ratvijitvech, P. Guiglion, M. A. Zwijnenburg, D. J. Adams and A. I. Cooper, *J. Am. Chem. Soc.*, 2015, **137**, 3265-3270.